Available online at www.sciencedirect.com
ScienceDirect
Tetrahedron
Tetrahedron 63 (2007) 8794–8800

Glycine and L-glutamic acid-based dendritic gelators

Wu-Song Li,[a] Xin-Ru Jia,[a,*] Bing-Bing Wang,[a] Yan Ji[a] and Yen Wei[b,*]

[a]*Department of Polymer Science and Engineering and Key Laboratory of Polymer Chemistry and Physics of the Ministry of Education, College of Chemistry and Molecular Engineering, Peking University, Beijing 100871, China*
[b]*Department of Chemistry, Drexel University, Philadelphia, PA 19104, USA*

Received 16 April 2007; revised 8 June 2007; accepted 12 June 2007
Available online 16 June 2007

Abstract—Novel dendrons based on glycine and L-glutamic acid from the first generation (**G1**) to the third generation (**G3**) were synthesized and studied for their gelation properties by using transmission electron microscopy (TEM), atomic force microscopy (AFM), fluorescence, IR, circular dichroism (CD), and ^{1}H NMR spectroscopy. It was found that the gelation capability of these dendrons increased from the first generation (**G1**) to the third generation (**G3**), and that **G3** exhibited the highest efficiency in forming gels. Both the focal and peripheral groups of dendrons had great effects on the formation of organogels. Hydrogen bonding and π–π stacking interactions were proved to be the main driving forces to form the fibrous networks at low concentrations (0.5 wt %). Small-angle X-ray scattering (SAXS) and wide-angle X-ray diffraction (WAXD) measurements indicate that the xerogels of the second generation (**G2**) from ethyl acetate and ethanol, and **G3** xerogel from CH_2Cl_2 all display lamellar structures with the interlamellar spacing of ca. 36.0 Å for **G2** and 40.5 Å for **G3**, respectively.

1. Introduction

There has been increasing interest in the bottom-up strategy for self-assembly of dendritic molecules in recent years.[1] As one type of the most intriguing supramolecular building blocks, gelators[2] have attracted considerable attention of chemists and biochemists owing to their potential applications in cosmetics, catalysis, drug delivery, food, tissue engineering, textile, paper, and photographic industry.[3] Dendritic molecules, which locate somewhere between small organic molecules and polymers, are of particular importance in gel technology because they combine the advantages of well-defined structures and the capability of forming multiple non-covalent interactions.[4]

As early as 1986, Newkome and co-workers initiated the research field of dendritic gelators. They reported a series of arborol-shaped hydrogelators and presented the structural effects on gelation by changing the linkers of two arborols.[5] Aida and co-workers reported the first example of dendritic organogel in 2000 by using Fréchet-type dendrons with a peptide-core.[6] Great emphasis has been placed on the design of dendritic gelators that are capable of gelling in various solvents from then on. For example, Smith and co-workers reported a series of one-component and two-component dendritic gelators.[7] They described in detail the effects of various factors on two-component gel-phase self-assembly, such as spacer chain,[7a] generation of dendrons and dendrimers,[7b] solvents,[7c] stereochemistry,[7d] ratio of two components,[7e] and peripheral groups.[7f] Majoral et al. synthesized thermoreversible hydrogels based on water-soluble phosphorus-containing dendrimers.[8] Kim et al. used amide dendrons and dendrimers with surface alkyl-[9a] and alkynyl-containing[9b] tails to form gel-phase materials in organic solvents. Grinstaff et al. reported the synthesis of dendritic-linear hybrid polymers containing methacrylate units on the periphery.[10] They found that the double bonds could be crosslinked via in-situ photopolymerization to form hydrogels. In addition, Stupp and co-workers developed a series of rod-coil hybrid dendritic organogelators,[11] some of which could self-assemble into nanoribbons with potential applications in electronic devices.[11a,b]

In recent years, dendritic gelators based on natural amino acids have been developed into a very active field for the advantages of biocompatibility, biodegradability, and less toxicity possessed by dendritic peptide structures.[12] For example, Smith et al. synthesized a series of dendritic gelators on the basis of L-lysine.[7] Moreover, L-lysine-based dendritic hydrogelators were also described by Stupp and co-workers.[13] They announced that the hydrogels with unique properties could be used in cell and tissue engineering.[13a] However, most of the peptide dendritic gelators are constructed from one kind of amino acid. Interestingly, if two or more types of amino acids are used in the construction of dendritic gelators, the structural diversity (similar to the sequence variety of natural proteins and peptides) of gelators could be resulted. As an example, Chow and Zhang[14] synthesized a series of dendritic gelators on the basis of three

Keywords: Glycine; L-Glutamic acid; Dendritic gelators; Self-assembly.
* Corresponding authors. Tel.: +86 10 62752102; fax: +86 10 62751708 (X.-R.J.); tel.: +1 215 895 2652; fax: +1 215 895 1265 (Y.W.); e-mail addresses: xrjia@pku.edu.cn; weiyen@drexel.edu

0040–4020/$ - see front matter © 2007 Elsevier Ltd. All rights reserved.
doi:10.1016/j.tet.2007.06.028

different amino acids—alanine, phenylalanine, and valine. They found that the gelation properties were influenced by the layer sequence of the amino acids.[14a] We previously reported a **G3** dendron based on two natural amino acids—glycine (Gly) and L-aspartic acid (Asp), which could act as an effective dendritic organogelator,[15] however, it only gelled in mixed solvents. In order to seek more efficient dendritic gelators and further elucidate the structural effects on gelation properties, L-aspartic acid was replaced by L-glutamic acid (Glu) in the structure of newly synthesized dendrons. As expected, the Gly–Glu dendrons showed stronger gelation ability than the Gly–Asp ones although their structures were quite similar. Herein, we report the gelation properties of Gly–Glu dendrons from the first to third generation (**G1** to **G3**) and the deprotected dendrons with focal $-NH_2$ or peripheral –COOH groups, that is, **G1-NH$_2$**, **G2-NH$_2$**, **G1-COOH**, and **G2-COOH** in various solvents, respectively. The structures and driving forces of the gel-phase assemblies are also described in this article.

2. Results and discussion

2.1. Synthesis and characterization

The synthesis of Gly–Glu dendrons from **G1** to **G3** (Scheme 1) has been previously reported.[16] **G1** was synthesized by the coupling reaction of Boc-glycine

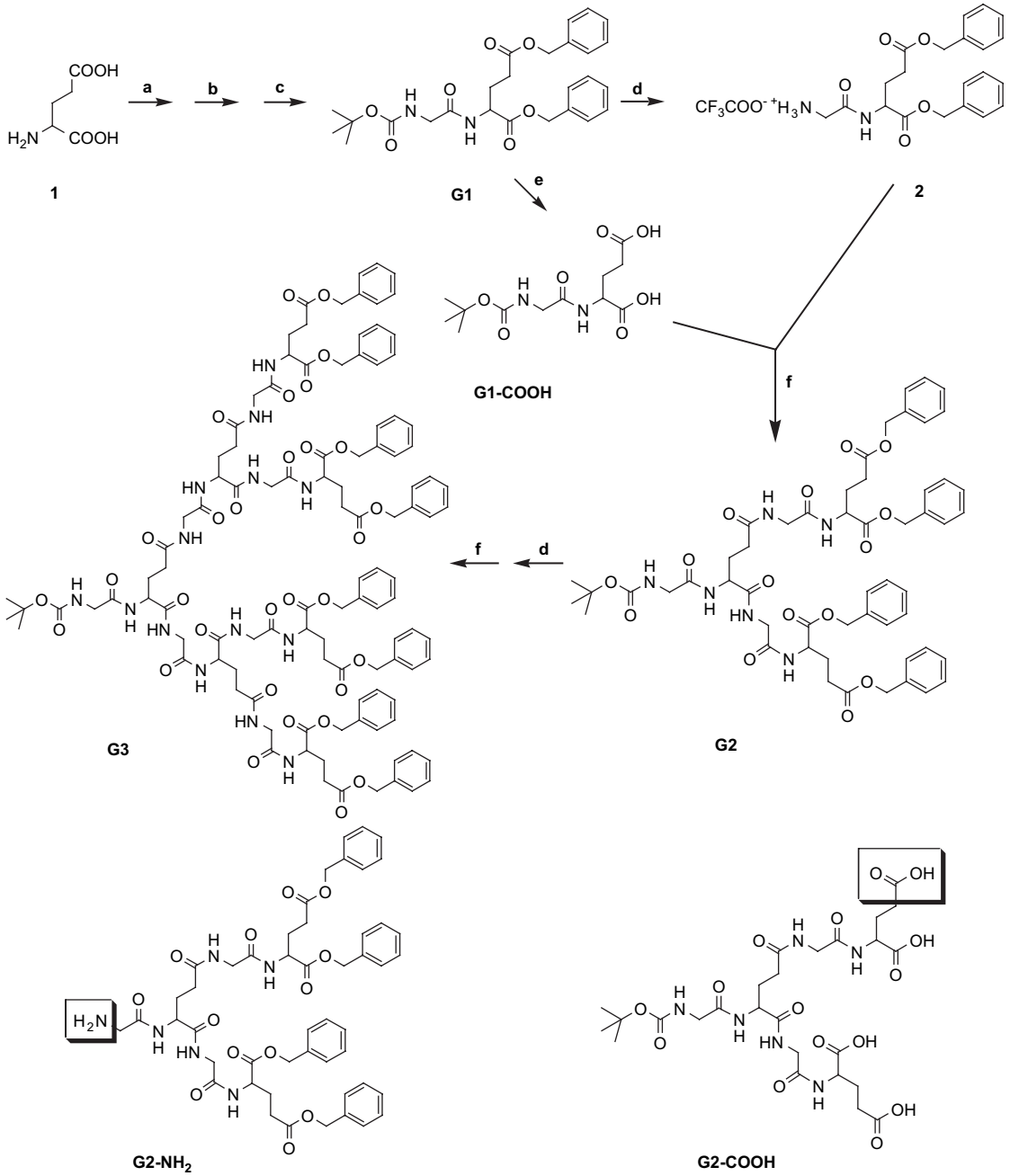

Scheme 1. Structures and convergent synthesis of Gly–Glu dendrons. Reagents and conditions: (a) *p*-toluenesulfonic acid, benzene, benzyl alcohol, reflux; (b) CH_3OH, KOH; (c) Boc-glycine, DCC, −10 °C; (d) TFA, CH_2Cl_2; (e) Pd–C, H_2, ethanol; (f) DCC, **G1-COOH**, *N*-methyl-morpholine, −10 °C.

(Boc=*tert*-butoxycarbonyl) and benzyl-protected L-glutamic acid in the presence of dicyclohexylcarbodiimide (DCC), while the benzyl-protected L-glutamic acid was prepared from the esterification of L-glutamic acid (**1**, Scheme 1) with benzyl alcohol. **G2** and **G3** were synthesized by repeating the following convergent reactions: removing the Boc group of the lower generation dendrons with trifluoroacetic acid (TFA), and then coupling the resulted *N*-deprotected intermediate (e.g., **2**, Scheme 1) with **G1-COOH** (Scheme 1) derived from **G1** by Pd-catalyzed hydrogenation. The yields of **G1**, **G2**, and **G3** were 80, 60, and 50%, respectively. The chemical structures and purities of the dendrons have been verified by elemental analysis, ^{1}H NMR, ^{13}C NMR, FTIR, MALDI-TOF MS. In order to better understand the structural effects on the gelation properties, the first- and second-generation deprotected dendrons with focal $-NH_2$ or peripheral –COOH groups, such as **G2-NH$_2$** and **G2-COOH** (Scheme 1) were also prepared.

2.2. Gelation properties

Table 1 summarizes the gelation properties of **G1**–**G3** Gly–Glu dendrons. As shown in Table 1, **G1** did not gel in any tested solvents, whereas **G2** and **G3** were efficient organogelators. Specifically, **G3** displayed stronger gelation ability than **G2**. It could gel in various organic solvents at very low concentrations. For example, the minimum gel concentration (MGC) of **G3** in methanol was 4 mg/mL (one **G3** molecule could entrap about 1.3×10^4 methanol molecules). It is interesting to note that the gelation ability increases from **G1** to **G3**, which indicates a positive dendritic effect that the dendrons of higher generations are more efficient to form gels. Smith and co-workers have first reported the positive dendritic effect on the gelation of L-lysine-based dendrimers.[7g] They ascribed it to the more extensive hydrogen-bonding interaction among the amide groups in dendrimers with higher generations. In our case, **G3** with more dendritic branches could provide more hydrogen bonding and π–π stacking sites, enhanced hydrophobic interaction and van der Waals force, all of which would strengthen the gel-phase self-assembly.[17] This result is also consistent with that reported by Jang et al. They found that the **G2** and **G3** Fréchet-type dendrons with a dipeptide group at the focal point[6,18] were efficient in gelation because the bulky dendritic wedges favored the stabilization of hydrogen bonds,[6] whereas the first-generation dendron did not form gels but only gave a crystalline solid.

In addition, the deprotected dendrons, i.e., **G1-NH$_2$**, **G1-COOH**, **G2-NH$_2$**, and **G2-COOH** did not form gels. This result is attributed to the absence of the Boc group or benzene rings, indicating the important roles of hydrophobic and π–π stacking interactions in gelation. It will be further discussed in the section of 'gelation mechanism'.

Moreover, **G2** could also gel in mixed solvents, such as the mixture of cyclohexane and ethyl acetate (4/1, v/v) and the mixture of diethyl ether and methanol (9/1, v/v). In comparison with Gly–Asp dendrons, of which only the third generation could gel in mixed solvents (not gel in single solvent),[15] Gly–Glu dendrons appear to be more efficient gelators. From the structural point of view, **G2** and **G3** Gly–Glu dendrons possess more hydrophobic domains than Gly–Asp dendrons because there is one more methylene group in the structure of L-glutamic acid. These additional hydrophobic domains might provide stronger hydrophobic interaction and an optimum balance of multiple non-covalent interactions, which led to efficient gelation. Suzuki and co-workers have reported a coincident conclusion that an appropriate hydrophilic–hydrophobic balance was important for effective gelation of L-lysine-based low-molecular mass organogelator (LMOG).[19]

It should be noted that Liu et al. recently reported the ultrasound induced gelation of a glutamic dendron.[20] The small dendritic molecule could form organogels under ultrasound in mixed solvents. Notably, we have also observed the effect of ultrasound on gelation: **G2** and **G3** Gly–Glu dendrons could gel in both single and mixed solvents either by heating or under ultrasound.

Table 1. Gelation properties of Gly–Glu dendrons in various solvents at 20 °C[a,b]

Solvents	G1	G2	G3
MeOH	—	OG (800)	OG (4)
EtOH	—	TG (18)	OG (16)
^{i}PrOH	—	TG (25)	OG (5)
^{i}BuOH	—	TG (35)	OG (17)
Acetone	—	—	OG (4)
THF	—	—	TG (15)
AcOEt	—	OG (50)	OG (13)
Ethylether	—	OG (5)	—
$CHCl_3$	—	—	CG (22)
CH_2Cl_2	—	—	CG (11)

[a] —: Nongelation at concentration below 100 mg/mL. The value in parentheses is the minimum gel concentration (MGC, mg/mL) for gelation at 20 °C.
[b] OG: opaque gel; TG: translucent gel; CG: clear transparent gel.

2.3. Morphology and structure analysis

Transmission electron microscopy (TEM) images of **G2** xerogel from ethyl acetate (Fig. 1(a)) and **G3** xerogel from ethanol (Fig. 1(b)) show that the dendrons self-assemble into fibrous network with the diameters no more than 100 nm. Interestingly, **G3** xerogels from other solvents, such as acetone and CH_2Cl_2, exhibit different morphologies. As shown in Figure 1(c), a tangled fibrous network with the fiber width ranging from 100 nm to 500 nm is observed when **G3** gels in acetone. The AFM image of **G3** xerogel from CH_2Cl_2 (Fig. 1(d)) reveals that fibrous bundles with a width of ca. 1 μm are formed due to the intertwining of thinner fibers.

In order to explore the possibility of chiral structure of the gel, circular dichroism (CD) spectra of **G3** gel in ethanol (Fig. 2) were recorded. Ordinarily, when the chromophoric moieties self-organize into chiral or helical aggregates, the Cotton effect would appear.[7b] The solution of **G3** did not show any CD signal but the **G3** gel gave a strong peak around 220 nm that ascribed to the amide groups[7b] of the dendritic peptide (Fig. 2(a)). Variable-temperature CD spectra of **G2** gel in ethanol exhibit that the signal intensity decreases with increasing temperature (Fig. 2(b)), indicating the CD signals should be attributed to the chiral organization in the gel-phase assemblies rather than the chirality of the molecules, though chiral morphology is not observed by TEM and AFM.

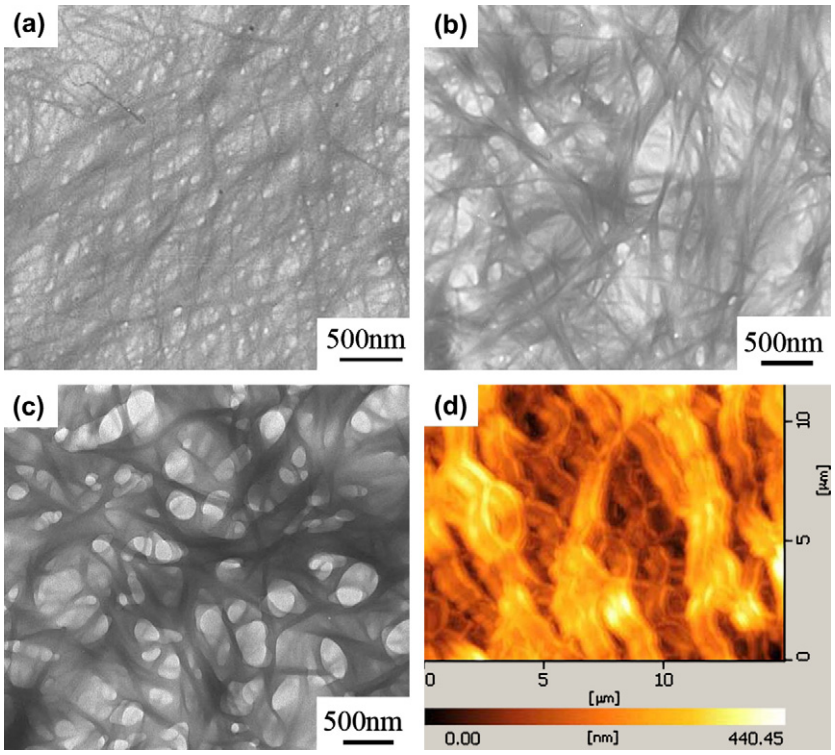

Figure 1. TEM images of gels prepared from **G2** in ethyl acetate (a), and **G3** in ethanol (b) and acetone (c) and AFM image of gel prepared from **G3** in CH_2Cl_2 (d).

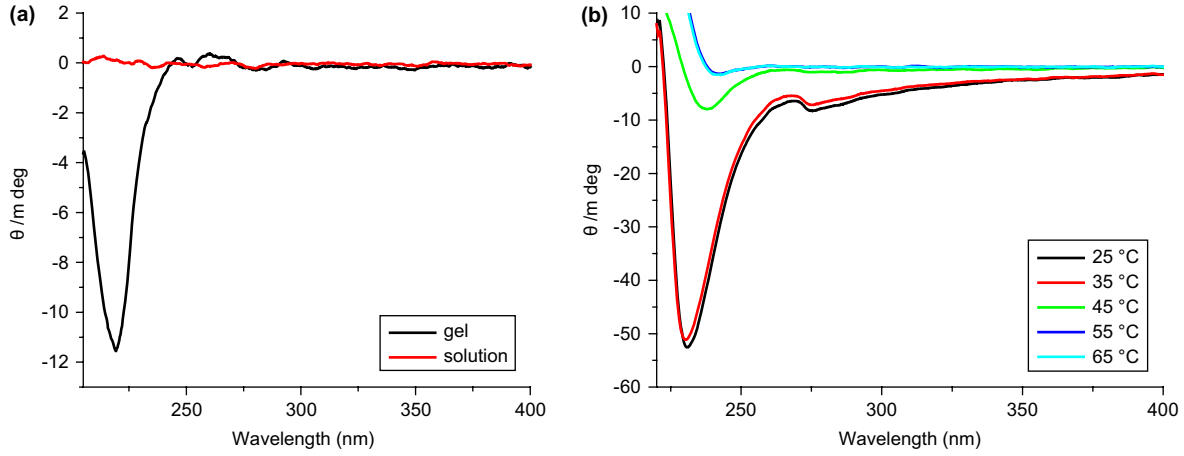

Figure 2. CD spectra (a) of **G3** in ethanol; dendritic gel (4 mg/mL; black line) and nongelled solution (0.1 mg/mL; red line); variable-temperature CD spectra (b) of dendritic gel from **G2** in ethanol (50 mg/mL; from 25 to 65 °C).

Two-dimensional (2D) wide-angle X-ray diffraction (WAXD) and small-angle X-ray scattering (SAXS) were carried out on gels and xerogels in order to reveal the packing patterns of the assemblies. No diffraction was detected for gels presumably because of strong scattering from the solvents. The WAXD pattern of **G2** xerogel from ethyl acetate (Fig. 3(a)) shows the diffraction peaks corresponding to *d* spacings of 35.5, 18.7, 11.7, 9.2, and 7.2 Å, respectively. The *d* values are in the ratio of 1:1/2:1/3:1/4:1/5, suggesting an ordered lamellar structure with an interlamellar spacing of 35.5 Å. **G2** xerogel from ethanol displays the same lamellar structure with an interlamellar spacing of 36.4 Å. In addition, the SAXS pattern (Fig. 3(b)) indicates that **G3** dendron in CH_2Cl_2 also self-assemble into a lamellar structure with an interlamellar spacing of 40.5 Å.

2.4. Gelation mechanism

Variable-temperature ^{1}H NMR spectra (Fig. 4) were employed to reveal the driving effect of hydrogen bonding in gelation. **G3** was dissolved in $CDCl_3$ and ^{1}H NMR measurements were performed at 24, 35, 45 , and 55 °C, respectively, with one sample at the concentration of 13 mg/mL. The $CDCl_3$ solution of **G3** was a 'sol-type' solution rather than a rigid gel because the gel-phase samples could not give ^{1}H NMR signals due to the immobilization of the dendritic molecules in the assembled networks. The ^{1}H NMR peaks in the range of 5–9 ppm correspond to the protons of amide groups in the peptide blocks, except that the strongest peak around 7.30 ppm is attributed to the protons of benzene rings and the peak at ca. 7.26 ppm is attributed to the protons of

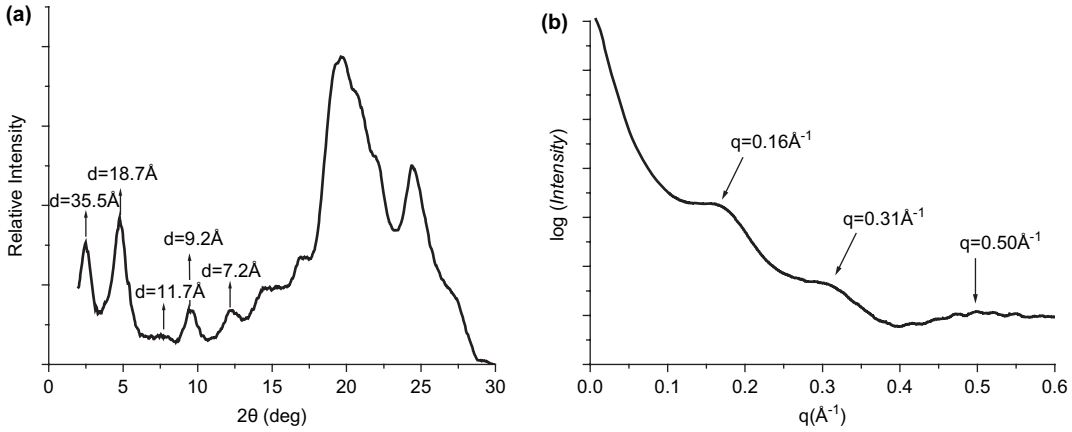

Figure 3. WAXD pattern (a) of **G2** xerogel from ethyl acetate and SAXS pattern (b) of **G3** xerogel prepared from CH_2Cl_2.

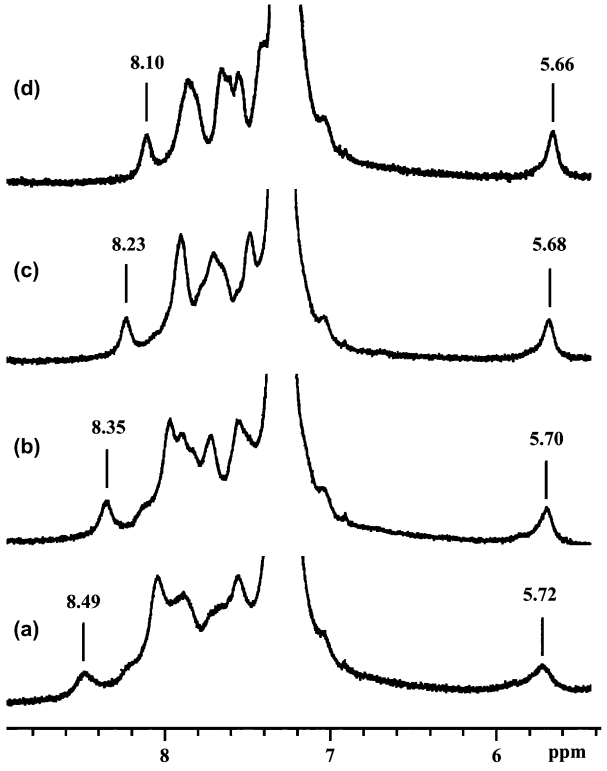

Figure 4. Variable-temperature ^{1}H NMR spectra of dendritic gel formed by **G3** in $CDCl_3$ (13 mg/mL) measured at 24 °C (a), 35 °C (b), 45 °C (c) and 55 °C (d).

incompletely deuterium-replaced solvent $CHCl_3$. As shown in Figure 4, up-field shifts of amide group protons were observed as the temperature was increased. For example, the peaks at 8.49 ppm and 5.72 ppm at 24 °C shifted to 8.11 ppm and 5.66 ppm at 55 °C, which indicated the weakening of hydrogen bonds of amide groups and implied that the hydrogen-bonding interaction played a key role in mediating the gel-phase assembly.[7g]

The driving effect of hydrogen bonding in gelation could also be proved by using FTIR spectroscopy. Figure 5 shows the FTIR spectra of **G3** solid and **G3** xerogel formed from $CHCl_3$. **G3** solid exhibits characteristic bands of stretching vibration of N–H at 3303 cm^{-1} and C═O at 1655 cm^{-1} (amide I) and blending vibration of N–H at 1536 cm^{-1} (amide II), while the gel sample shows that the vibration bands shift to 3290 cm^{-1} (N–H stretching), 1632 cm^{-1} (amide I) and 1545 cm^{-1} (amide II), respectively, indicating the presence of hydrogen bonding interaction in the gel-phase assembly. Such a result is consistent with that reported by Suzuki et al.,[21] where they found similar IR vibration band shifts in the LMOG based on L-valine and L-isoleucine.

Fluorescence spectroscopy with pyrene as a probe was employed to explore the contribution of hydrophobic interaction to gelation. It is well known that the intensity ratio I_1/I_3 of pyrene emissions is an indicator for the polarity of the microenvironment in the solution (I_1 and I_3 represent the intensities of the first and the third peaks of the quintuple peaks in the emission of pyrene, respectively).[22] In our study, the ratio I_1/I_3 decreased with the increase of **G2** concentration in ethanol, indicating that the nonpolar domains formed owing to the hydrophobic interaction[22] among hydrophobic units and the π–π stacking interaction[15] among peripheral benzene rings of the dendrons. In addition, the WAXD diffraction peak appearing at 24.6° 2θ-angle (Fig. 3(a)) could also prove the existence of π–π stacking in the gel-phase material according to Harris and co-workers.[23]

3. Conclusions

In summary, dendrons of different generations (**G1**–**G3**) with glycine and L-glutamic acid as building blocks have been successfully synthesized and their gelation properties were investigated. **G2** and **G3** dendrons are capable of forming gels in various organic solvents including single and mixed solvents, and **G3** dendron is a more efficient dendritic gelator than **G2**. Variable-temperature ^{1}H NMR, fluorescence and FTIR spectra reveal that hydrogen bonding, π–π stacking and hydrophobic interaction are the main driving forces for the fibrous assemblies. WAXD and SAXS measurements indicate that **G2** xerogels (from ethyl acetate and ethanol) and **G3** xerogel (from CH_2Cl_2) all display lamellar structures with the interlamellar spacing of ca. 36.0 Å for **G2** and 40.5 Å for **G3**, respectively. The investigation of structural effects on the gelation behavior of natural amino acids-based dendritic gelators may provide

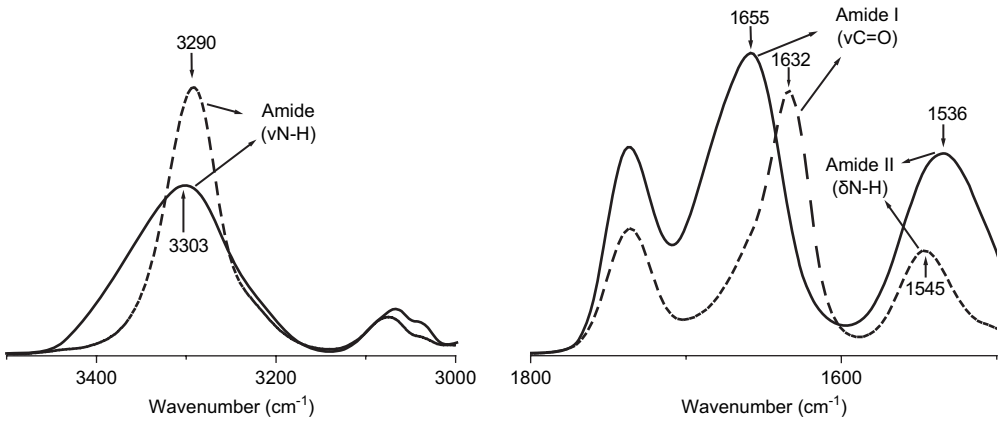

Figure 5. FTIR spectra of **G3** solid (solid line) and **G3** xerogel formed from $CHCl_3$ (dashed line).

immense opportunities for the bottom-up fabrication of supramolecular biomaterials.

4. Experimental

4.1. Materials and synthesis

Unless stated otherwise, all reagents and common solvents were obtained from commercial sources and used as received. HPLC grade ethanol used for circular dichroism and fluorescence spectroscopy measurements was purchased from Tianjin Shield Company (China). All the dendritic molecules were synthesized according to the method reported previously.[16]

4.2. Gelation experiments

A certain amount of dendritic gelator was mixed with a measured volume of pure solvent in a septum-capped vial with a diameter of 1 cm and then heated in an oil bath for 5 min. The mixture was sonicated under ultrasound at ambient temperature for 30 min and then was allowed to stand for 24 h. A stable gel was formed if a 'solid-like' phase (i.e., no flow) was observed when inverting the vial. Some samples could form gels directly under ultrasound and did not need to be heated. MGC was determined by weighing up a minimum amount of dendritic gelator needed for the formation of a stable gel.

4.3. Measurements

4.3.1. Transmission electron microscopy. TEM measurements were performed on a JEM-100 CXII microscope, being operated at an acceleration voltage of 100 kV. Gel samples used for TEM were loose gels and dropped on carbon-coated formvar 200 mesh copper grids. Excess gels were removed leaving some small patches of gels on the grids after 1 min. The solvents evaporated spontaneously at room temperature before measurements.

4.3.2. Atomic force microscopy. Tapping-mode AFM measurements were performed using a SPA-400 Multimode AFM and SPI3800N Probe Station. Loose gel samples were dropped on freshly cleaved mica surface and solvents evaporated spontaneously at room temperature before imaging.

4.3.3. Circular dichroism measurements. CD spectra of gels and solutions were recorded on a Jasco J-810 spectropolarimeter equipped with a Julabo F25 thermostatic apparatus. The samples were dropped into or prepared in a quartz cuvette with a path length of 0.1 mm.

4.3.4. Variable-temperature ^{1}H NMR measurements. Variable-temperature ^{1}H NMR measurements were performed on a Varian Mercury 300 MHz spectrometer using $CDCl_3$ as solvent and tetramethylsilane (TMS) as an internal standard. The sample of **G3** in $CDCl_3$ with a concentration of 13 mg/mL was heated and left for 24 h before measuring. The temperature of sample was increased from 24 to 55 °C and kept at 24, 35, 45, and 55 °C for 10 min, respectively, during the measurement.

4.3.5. FTIR spectroscopy. FTIR spectra were obtained on a Nicolet Magna-IR 750 spectrometer and the samples were planished on the surface of a diamond-sheet before scanning for 64 times. The solvent of the gel sample evaporated spontaneously at room temperature before measurements.

4.3.6. Fluorescence spectroscopy. The fluorescence spectroscopy measurements were carried out on a Hitachi F-4500 fluorescence spectrophotometer at room temperature. The different amount of **G3** samples were dissolved in a pyrene ethanol solution (5×10^{-6} M) and left for 24 h before measurements. The excitation wavelength was 335 nm and no excimer peak was observed in the emission spectra.

4.3.7. Wide-angle X-ray diffraction. 2D WAXD measurements were performed on a Bruker D8 Discover diffractometer with GADDS as a 2D detector. Diffraction patterns were recorded in a transmission mode at room temperature employing Cu Kα radiation (λ=0.154 nm) and the air scattering was subtracted from the sample patterns. The gel samples were xerogels with the solvents being taken out in vacuo at room temperature.

4.3.8. Small-angle X-ray scattering. SAXS measurements were performed on equipment with a SAXSess camera (Anton-Paar, Graz, Austria), which is connected with an X-ray generator (Philips) operating at 40 kV and 50 mA employing Cu Kα radiation (λ=0.154 nm). The 1D scattering function ($\log I(q)$) was obtained by integrating the 2D

scattering pattern, which was recorded on an imaging-plate detector (Perkin–Elmer) using SAXSQuant software (Anton-Paar, Graz, Austria). The xerogel sample for SAXS was prepared in a similar way to the samples for WAXD. It was sealed in a solid sample holder and the blank scattering was subtracted from the sample scattering to obtain the xerogel exact diffraction pattern.

Acknowledgements

This work was supported by the National Natural Science Foundation of China (NSFC no. 20574001 and 20640420562 to X.-R.J). We thank Prof. Naiheng Song for the useful discussions.

References and notes

1. (a) Fréchet, J. M. J. *Science* **1994**, *263*, 1710–1715; (b) Zeng, F. W.; Zimmerman, S. C. *Chem. Rev.* **1997**, *97*, 1681–1712; (c) Fischer, M.; Vögtle, F. *Angew. Chem., Int. Ed.* **1999**, *38*, 884–905; (d) Zimmerman, S. C.; Lawless, L. J. *Top. Curr. Chem.* **2001**, *217*, 95–120; (e) Percec, V.; Glodde, M.; Bera, T. K.; Miura, Y.; Shiyanovskaya, I.; Singer, K. D.; Balagurusamy, V. S. K.; Heiney, P. A.; Schnell, I.; Rapp, A.; Spiess, H.-W.; Hudson, S. D.; Duan, H. *Nature* **2002**, *419*, 384–387; (f) Smith, D. K.; Hirst, A. R.; Love, C. S.; Hardy, J. G.; Brignell, S. V.; Huang, B. *Prog. Polym. Sci.* **2005**, *30*, 220–293.
2. (a) Terech, P.; Weiss, R. G. *Chem. Rev.* **1997**, *97*, 3133–3159; (b) van Esch, J. H.; Feringa, B. L. *Angew. Chem., Int. Ed.* **2000**, *39*, 2263–2266; (c) Gronwald, O.; Snip, E.; Shinkai, S. *Curr. Opin. Colloid Interface Sci.* **2002**, *7*, 148–156; (d) Estroff, L. A.; Hamilton, A. D. *Chem. Rev.* **2004**, *104*, 1201–1217.
3. (a) Peppas, N. A.; Huang, Y.; Tottes-Lugo, M.; Ward, J. H.; Zhang, J. *Annu. Rev. Biomed. Eng.* **2000**, *2*, 9–29; (b) Langer, R. *Acc. Chem. Res.* **2000**, *33*, 94–101; (c) Lee, K. Y.; Mooney, D. J. *Chem. Rev.* **2001**, *101*, 1869–1879; (d) Abdallah, D. J.; Weiss, R. G. *Adv. Mater.* **2000**, *12*, 1237–1247; (e) Kato, T. *Science* **2002**, *295*, 2414–2418.
4. Hirst, A. R.; Smith, D. K. *Top. Curr. Chem.* **2005**, *256*, 237–273.
5. (a) Newkome, G. R.; Baker, G. R.; Saunders, M. J.; Russo, P. S.; Gupta, V. K.; Yao, Z.-q.; Miller, J. E.; Bouillion, K. *J. Chem. Soc., Chem. Commun.* **1986**, 752–753; (b) Newkome, G. R.; Baker, G. R.; Arai, S.; Saunders, M. J.; Russo, P. S.; Theriot, K. J.; Moorefield, C. N.; Rogers, L. E.; Miller, J. E.; Lieux, T. R.; Murray, M. E.; Phillips, B.; Pascal, L. *J. Am. Chem. Soc.* **1990**, *112*, 8458–8465; (c) Newkome, G. R.; Moorefield, C. N.; Baker, G. R.; Behera, R. K.; Escamillia, G. H.; Saunders, M. J. *Angew. Chem., Int. Ed. Engl.* **1992**, *31*, 917–919; (d) Newkome, G. R.; Lin, X.; Yaxiong, C.; Escamilla, G. H. *J. Org. Chem.* **1993**, *58*, 3123–3129; (e) Yu, K. H.; Russo, P. S.; Younger, L.; Henk, W. G.; Hua, D. W.; Newkome, G. R.; Baker, G. *J. Polym. Sci., Polym. Phys.* **1997**, *35*, 2787–2793.
6. Jang, W.-D.; Jiang, D.-L.; Aida, T. *J. Am. Chem. Soc.* **2000**, *122*, 3232–3233.
7. (a) Hirst, A. R.; Smith, D. K.; Feiters, M. C.; Geurts, H. P. M. *Langmuir* **2004**, *20*, 7070–7077; (b) Hirst, A. R.; Smith, D. K. *Org. Biomol. Chem.* **2004**, *2*, 2965–2971; (c) Hirst, A. R.; Smith, D. K. *Langmuir* **2004**, *20*, 10851–10857; (d) Hirst, A. R.; Smith, D. K.; Feiters, M. C.; Geurts, H. P. M. *Chem.—Eur. J.* **2004**, *10*, 5901–5910; (e) Hirst, A. R.; Smith, D. K.; Feiters, M. C.; Geurts, H. P. M.; Wright, A. C. *J. Am. Chem. Soc.* **2003**, *125*, 9010–9011; (f) Hardy, J. G.; Hirst, A. R.; Smith, D. K.; Brennan, C.; Ashworth, I. *Chem. Commun.* **2005**, 385–387; (g) Love, C. S.; Hirst, A. R.; Chechik, V.; Smith, D. K.; Ashworth, I.; Brennan, C. *Langmuir* **2004**, *20*, 6580–6585; (h) Partridge, K. S.; Smith, D. K.; Dykes, G. M.; McGrail, P. T. *Chem. Commun.* **2001**, 319–320; (i) Huang, B.; Hirst, A. R.; Smith, D. K.; Castelletto, V.; Hamley, I. W. *J. Am. Chem. Soc.* **2005**, *127*, 7130–7139.
8. (a) Marmillon, C.; Gauffre, F.; Gulik-Krzywicki, T.; Loup, C.; Caminade, A.-M.; Majoral, J.-P.; Vors, J.-P.; Rump, E. *Angew. Chem., Int. Ed.* **2001**, *40*, 2626–2629; (b) El-Ghzaoui, A.; Gauffre, F.; Caminade, A.-M.; Majoral, J.-P.; Lannibois-Drean, H. *Langmuir* **2004**, *20*, 9348–9353.
9. (a) Kim, C.; Kim, K. T.; Chang, Y.; Song, H. H.; Cho, T.-Y.; Jeon, H.-J. *J. Am. Chem. Soc.* **2001**, *123*, 5586–5587; (b) Kim, C.; Lee, S. J.; Lee, I. H.; Kim, K. T.; Song, H. H.; Jeon, H.-J. *Chem. Mater.* **2003**, *15*, 3638–3642.
10. (a) Carnahan, M. A.; Middleton, C.; Kim, J.; Kim, T.; Grinstaff, M. W. *J. Am. Chem. Soc.* **2002**, *124*, 5291–5293; (b) Luman, N. R.; Smeds, K. A.; Grinstaff, M. W. *Chem.—Eur. J.* **2003**, *9*, 5618–5626.
11. (a) Messmore, B. W.; Hulvat, J. F.; Sone, E. D.; Stupp, S. I. *J. Am. Chem. Soc.* **2004**, *126*, 14452–14458; (b) Sone, E. D.; Zubarev, E. R.; Stupp, S. I. *Angew. Chem., Int. Ed.* **2002**, *41*, 1705–1709; (c) Zubarev, E. R.; Pralle, M. U.; Sone, E. D.; Stupp, S. I. *J. Am. Chem. Soc.* **2001**, *123*, 4105–4106; (d) Zubarev, E. R.; Pralle, M. U.; Sone, E. D.; Stupp, S. I. *Adv. Mater.* **2002**, *14*, 198–203; (e) Li, L.; Beniash, E.; Zubarev, E. R.; Xiang, W.; Rabatic, B. M.; Zhang, G.; Stupp, S. I. *Nat. Mater.* **2003**, *2*, 689–694.
12. (a) Kim, Y.; Zimmerman, S. C. *Curr. Opin. Chem. Biol.* **1998**, *2*, 733–742; (b) Cloninger, M. J. *Curr. Opin. Chem. Biol.* **2002**, *6*, 742–748; (c) Crespo, L.; Sanclimens, G.; Pons, M.; Giralt, E.; Royo, M.; Albericio, F. *Chem. Rev.* **2005**, *105*, 1663–1681.
13. (a) Stendahl, J. C.; Li, L.; Claussen, R. C.; Stupp, S. I. *Biomaterials* **2004**, *25*, 5847–5856; (b) Klok, H.-A.; Hwang, J. J.; Hartgerink, J. D.; Stupp, S. I. *Macromolecules* **2002**, *35*, 6101–6111.
14. (a) Chow, H.-F.; Zhang, J. *Chem.—Eur. J.* **2005**, *11*, 5817–5831; (b) Chow, H.-F.; Zhang, J. *Tetrahedron* **2005**, *61*, 11279–11290.
15. Ji, Y.; Luo, Y.-F.; Jia, X.-R.; Chen, E.-Q.; Huang, Y.; Ye, C.; Wang, B.-B.; Zhou, Q.-F.; Wei, Y. *Angew. Chem., Int. Ed.* **2005**, *44*, 6025–6029.
16. Li, W.-S.; Ji, Y.; Jia, X.-R.; Wang, B.-B.; Wei, Y. *Acta Polym. Sin.* **2006**, 712–716.
17. (a) Whitesides, G. M.; Grzybowski, B. *Science* **2002**, *295*, 2418–2421; (b) Hamley, I. W. *Angew. Chem., Int. Ed.* **2003**, *42*, 1692–1712.
18. Jang, W.-D.; Aida, T. *Macromolecules* **2003**, *36*, 8461–8469.
19. Suzuki, M.; Yumoto, M.; Kimura, M.; Shirai, H.; Hanabusa, K. *Chem.—Eur. J.* **2003**, *9*, 348–354.
20. Li, Y.; Wang, T.; Liu, M. *Tetrahedron* **2007**, *63*, 7468–7473.
21. Suzuki, M.; Sato, T.; Kurose, A.; Shirai, H.; Hanabusa, K. *Tetrahedron Lett.* **2005**, *46*, 2741–2745.
22. Ganesh, S.; Prakash, S.; Jayakumar, R. *Biopolymers* **2003**, *70*, 346–354.
23. Hu, J.; Zhang, D.; Jin, S.; Cheng, S. Z. D.; Harris, F. W. *Chem. Mater.* **2004**, *16*, 4912–4915.